Binding in clusters with closed-subshell atoms (alkaline-earth elements)

I.G. Kaplan,[1,2] Szczepan Roszak,[2,3] and Jerzy Leszczynski[2]

[1]Instituto de Investigaciones en Materiales, UNAM, Apartado Postal 70-360, 04510 Mexico, D.F., MEXICO

[2]The Computational Center for Molecular Structure and Interactions, Department of Chemistry, Jackson State University, P.O. Box 17910 J.R. Lynch Street, Jackson, Mississippi 39217, USA

[3]Institute of Physical and Theoretical Chemistry, Wroclaw University of Technology, Wyb. Wyspianskiego 27, 50-370 Wroclaw, Poland

Abstract

The study of the binding in clusters with closed subshell atoms is performed. The study is based on the accurate calculations of the Be_n, Mg_n, and Ca_n (n =2, 3) clusters at the Møller-Plesset electron correlation level (MP4) and the SCF level, using a reasonably large basis set [6-311 + G(3df)]. The 2-and 3-body decompositions of the interaction energy at the MP4 and SCF levels, the NBO population analysis and the electron density difference maps allow to elucidate the nature of bonding in alkaline-earth clusters

Contents

ADVANCES IN QUANTUM CHEMISTRY, VOLUME 40

0065-3276/01 $35.00

1 Introduction

Many definitions of the phenomenon of chemical bonding are used. One appropiate definition can be formulated in the following way:

chemical bonding is the attraction between atoms due to the redistribution (collectivization, charge transfer) of their valence electron density.

According to this definition, a two-atom molecule can be bound by a covalent bond (collectivization of valence electrons), by an ionic bond (charge transfer between atoms), and by so-called polar bond (intermediate case: collectivization + charge transfer), see also Ref.[1].

Compounds, constructed with atoms having closed electronic shells or subshells have no valence electrons and do not fulfil the chemical bond definition. A well known example is the noble-gas atoms. They are stabilized by the van der Waals (dispersion) forces. The van der Waals bond is caused by the quantum mechanical fluctuations in the electron density of interacting atoms. On an average, the atomic electron density is not changed. Thus, according to the definition above, the van der Waals bond cannot be attributed to chemical bonding but rather to physical bonding. The binding by the van der Waals forces is very weak in comparison with the chemical bonding. The weakest measured bond was found in He_2: the dissociation energy is $D_0 = 1.2$ mK or 2.38 o10^{-6} kcal/mol [2] (the well depth is larger and equals 0.02 kcal/mol). Even in bulk, the noble gas atoms have such small cohesive energy that can form solids only at low temperature and He remains liquid at all temperatures. This is a consequence of the closed-shell electronic structure of the noble gas elements.

On the other hand, the alkaline earth elements Be, Mg, Ca, etc. have a closed electronic subshell, $(ns)^2$, but form solids with quite large cohesive energy, see Table I. The cohesive energy in solid Be equals 3.32 eV/atom which is larger than that in solids of open one-valence ns shell atoms: Li (1.63 eV/atom) and Na (1.10 eV/atom).

The dimers of Be, Mg and Ca are very weakly bound by the electron correlation effects, at the self-consistent field (SCF) level they are not stable. The binding energy of alkaline earth dimers is only 2-4 times larger than that in Kr_2 and Xe_2 dimers. Thus, alkaline dimers can be attributed to the van der Waals molecules. The situation is changed in many-atom clusters, even in trimers (Table II). This is evidently a manifestation of the many-body effects. The crucial role of the 3-body forces in the stabilization of the Be_n clusters was revealed at the SCF level previously [3-5], and more recently was established at the Møller-Plesset perturbation theory level up to the fourth order (MP4) [6,7]. The study of binding in the Be_n clusters [8-10] reveals that the 3-body exchange forces are attractive and give an important contribution to

the attractive 2-body dispersion forces. At equilibrium distances, the latter are almost completely compensated by the repulsive 2-body exchange forces. This makes the role of 3-body exchange attraction even more important. In alkaline earths we meet with a many-body binding.

Table I: Some properties of alkaline earth atoms and solids.

	ATOMS			SOLID	
	Polarizability 10^{-24} cm^3 [a]	ΔE_{at}, kcal/mol [b]	$\langle r_{nl} \rangle$ [c]	E_c kcal/mol [d]	T_m K [d]
Be	5.6	$2s^2 \longrightarrow 2s2p \ ^3P^0$	$\langle r_{2s} \rangle = 2.65$	76.5	1562
		62.84			
Mg	10.6	$3s^2 \longrightarrow 3s3p \ ^3P^0$	$\langle r_{3s} \rangle = 3.25$	34.7	922
		62.47			
Ca	22.8 - 25.0	$4s^2 \longrightarrow 4s4d \ ^3D$	$\langle r_{4s} \rangle = 4.22$	42.5	1113
		43.34			
		$4s^2 \longrightarrow 4s3d \ ^3D$			
		58.14			

[a] Ref.23 [b] Ref.24 [c] Ref.25 [d] Ref.26

In order to reveal the details of binding in alkaline-earth clusters, it is important to carry out a comparative study of binding in clusters of Be, Mg, and Ca. There are many publications, in addition to those cited above, devoted to calculations of alkaline-earth clusters (see Refs. [10-21] and references therein). But in most of these studies, different computational approaches were applied to calculate the geometry and binding energy.

Table II: Comparision of our calculations with literature data for the equilibrium geometry, distances are in Å, energies are in kcal/mol, $E_b = -E_{int}$.

Refs.	Methods of calculation	Be_2		Be_3		Mg_2		Mg_3		Ca_2		Ca_3	
		r_0	E_b	r_0	E_b	r_0	E_b	r_0	E_b	r_0	E_b	r_0	E_b
[12]	CASSCF/CI	2.50	1.86	2.23	19.02								
[14]	MRCI			2.22	22.4			3.37	6.3				
[19]	MP4(SDTQ)			2.23	21.6								
[18]	Best estimations based on MP2-R12			2.20	26.9			3.37	8.0				
[11]	CI											3.97	11.53
[17]	MRCI											4.16	12.10
[27]	Experiment	2.45	2.26										
[28,29]	Experiment					3.89	1.16						
[22]	MP4(SDTQ)	2.56	1.83	2.24	25.90	3.92	1.09	3.32	7.12	4.56	2.14	4.12	11.66

The nature of binding in these clusters was not studied. The only exception, to the best of our knowledge, are two works by Bauschlicher et al.[10,11]. In their study of alkaline-earth clusters, the authors came to the conclusion that the promotion of atomic electrons from ns to np vacant orbitals, leading to hybridization, is a major mechanism responsible for the binding in alkaline-earth compounds. As shown below, this is not the case. The binding in alkaline-earth clusters has more complicated nature and depends on many factors.

Our analysis is based on accurate calculations performed in Ref.[22] at the Møller-Plesset electron correlation level of the interaction energy and its many-body decomposition for Be_n, Mg_n, and Ca_n (n= 2 and 3) clusters using a reasonably large basis set [6-311 + G (3df)]. All calculations were also carried out at the SCF level which allowed to study separately the SCF and electron correlation contributions and give a physical analysis of each term in the dimer and trimer energy decompositions.

2 Calculation scheme and its check

In variational methods, the interaction energy is not calculated directly even if the Møller-Plesset perturbation theory is used. We have to calculate the interaction energy at all calculation levels as a difference

$$E_{int}(N) = E(N) - NE_a \tag{1}$$

where E(N) is the total energy of cluster A_N; E_a is the atomic energy calculated at the same level of accuracy as E(N). For taking into account the basis set superposition error (BSSE), the atomic energy in Eq. (1) was calculated using the dimer basis set for N = 2 and the trimer basis set for N = 3.

All calculations in Ref.[22] were performed utilizing the Gaussian-98 code [30]. The potential energy scan was performed by means of the Møller-Plesset perturbation theory up to the fourth order (MP4) in the frozen core approximation. The electronic density distribution was studied within the population analysis scheme based on the natural bond orbitals [31,32]. A population analysis was performed for the SCF density and MP4(SDQ) generalized density determined applying the Z-vector concept [33].

We tested the quality of the calculations [22] by applying several different approaches. Firstly, the calculations were compared with Møller-Plesset calculations with no frozen core, $1s^2$ frozen, and $1s^22s^22p^6$ frozen core electrons for Be, Mg, and Ca clusters, respectively. The inclusion of more electron in the correlation energy calculations slightly lowers two- as well as three-body

interaction energies. The largest frozen space in the case of Ca clusters leads to total energy changes around 10% and does not affect the qualitative picture of the studied interactions. Test calculations were also performed by the coupled cluster method with single and double substitutions from the Hartree-Fock determinant and with inclusion of triple excitations non-iteratively, CCSD(T) [34,35]. The calculated interaction energies are within a few percent of those of Møller-Plesset calculations, indicating that the choice of the MP4(SDTQ) approach is well justified as a basic tool for the presented analysis.

In Table II the results of our calculations [22] of the equilibrium geometry and binding energy together with the published data are presented. A comparison with literature data indicates a quite satisfactory agreement. The values of the binding energy for the trimers Be_3 and Mg_3 are very close to the best estimations in Ref. [18].

In order to check the convergence of the MP perturbation series, the perturbation contributions $\varepsilon_{MP}^{(n)}$ to the interaction energy in each order have to be calculated:

$$\begin{aligned} \varepsilon_{MP}^{(2)} &= E_{int}^{MP2} - E_{int}^{SCF} \ , \\ \varepsilon_{MP}^{(3)} &= E_{int}^{MP3} - E_{int}^{MP2} \ , \\ \varepsilon_{MP}^{(4)} &= E_{int}^{MP4} - E_{int}^{MP3} \ , \end{aligned} \tag{2}$$

According to its definition, the correlation energy at the MP4 level is equal to

$$\Delta E^{corr} = E_{int}^{MP4} - E_{int}^{SCF} = \sum_{n=2}^{4} \varepsilon_{MP}^{(n)} \quad . \tag{3}$$

Let us express the MP series as the ratios to the second order contribution

$$\Delta E^{corr} = \varepsilon_{MP}^{(2)} \left(1 + \frac{\varepsilon_{MP}^{(3)}}{\varepsilon_{MP}^{(2)}} + \frac{\varepsilon_{MP}^{(4)}}{\varepsilon_{MP}^{(2)}} \right) \ . \tag{4}$$

At the equilibrium distance (Table III), the MP series (4) are the following:

$$\begin{aligned} Be_2 &: \ \varepsilon_{MP}^{(2)}(1 + 0.12 + 0.06) \ , \\ Mg_2 &: \ \varepsilon_{MP}^{(2)}(1 + 0.14 + 0.03) \ , \\ Ca_2 &: \ \varepsilon_{MP}^{(2)}(1 + 0.18 + 0.07) \ . \end{aligned} \tag{5}$$

Thus, the limitation of our calculation at the MP4 level looks quite justified. As shown in Ref. [22], the convergence is good at all calculated distances.

Table III: Interaction energy for dimers at the equilibrium distance at different levels of calculation, in kcal/mol.

Dimer	E_{int}^{SCF}	$\varepsilon_{MP}^{(2)}$	$\varepsilon_{MP}^{(3)}$	$\varepsilon_{MP}^{(4)}$	ΔE^{corr}	E_{int}^{MP4}
Be_2 $r_0 = 2.56$ Å	6.12	-6.71	-0.81	-0.43	-7.94	-1.83
Mg_2 $r_0 = 3.92$ Å	1.62	-2.34	-0.32	-0.06	-2.72	-1.09
Ca_2 $r_0 = 4.56$ Å	1.05	-2.56	-0.46	-0.17	-3.19	-2.14

The many-body decomposition of the interaction energy at different approximation is performed according to the general definitions, see Refs [36, 6]. For trimers we have only 2- and 3-body interaction energies. In the homoatomic case they are represented by the following formulae:

$$E_2(A_3) = \sum_{a<b} \varepsilon_{ab} \ , \tag{6}$$

$$\varepsilon_{ab} = E(ab) - 2E_a \tag{7}$$

where E(ab) is the total energy of two atoms at a particular distance they have in trimer abc. In the general case of a nonsymmetrical triangle, the sum (6) contains three different 2-body interaction energies.

The 3-body energy is defined as a difference

$$E_3(A_3) = E(A_3) - E_2(A_3) - 3E_a \tag{8}$$

where $E(A_3)$ is denoted as the total energy of trimer A_3.

The formulae (6)-(8) were applied for the calculations of the 2- and 3-body contributions to the interaction energy at the SCF and MP4 levels and for the decomposition of the electron correlation energy.

3 Discussion

3.1 Dimers

As was shown in Ref.[22], the interaction energy at the SCF level is positive for all three dimers at all distances. It is the electron correlation energy

that stabilizes the close-subshell-atoms dimers. The interaction energy at the equilibrium distances are presented in Table III. The equilibrium distance rises from $r_0 = 2.56$ Å for Be_2 to $r_0 = 4.56$ Å for Ca_2. The increase of the equilibrium distance in the row Be_2, Mg_2, and Ca_2 is well correlated with an increase in the average radius of the atomic valence shell (Table I). However, the binding energy does not have such monotonic behavior. The decrease of E_b from 1.83 kcal/mol for Be_2 to 1.09 kcal/mol for Mg_2 changes with an increase of E_b to 2.14 kcal/mol for Ca_2. The equilibrium distance for Ca_2 is very large (4.56 Å), and it could be expected that the bond will be weaker than in Mg_2. But this is not the case; the increase of the equilibrium distance compared with that in Mg_2 does not lead to weaker bond. It is explained by the smaller repulsive SCF energy and the larger correlation attraction at the equilibrium distances in the Ca_2 dimers, with respect to the Mg_2 dimer (see Table III). The same non-monotonic behavior takes place for the binding energy of the trimers: E_b = 25.9, 7.12, and 11.66 kcal/mol for Be_3, Mg_3, and Ca_3, respectively (Table II). It can be expected that this trend is also preserved in large clusters because in solid alkaline earths the cohesive energy and melting temperature show similar behavior (Table I).

The SCF interaction energy can be decomposed in different ways [36-38]. One possible decomposition is

$$E_{int}^{SCF} = \varepsilon_{el}^{(1)} + \varepsilon_{exch}^{(1)} + \Delta E_{ind.exch}^{def} \quad . \tag{9}$$

The electrostatics, $\varepsilon_{el}^{(1)}$, and exchange, $\varepsilon_{exch}^{(1)}$, energies correspond to the first order of the perturbation theory; so, they are defined in the undisturbed atomic wave functions. The third term, $\Delta E_{ind.exch}^{def}$, contains the induction interactions which cannot be separated from the exchange interactions. The induction forces polarize the SCF orbitals; accordingly, $\Delta E_{ind.exch}^{def}$ is defined on the deformed orbitals.

Atoms with closed subshells have no multipole moments and their electrostatic and induction interactions have a pure overlap origin; from which follows their short-range character. The main contribution to E_{int}^{SCF} gives the exchange interaction $\varepsilon_{exch}^{(1)}$. Between atoms with closed subshells, it is repulsive (as in the noble-gas atom systems). This determines the unstability of the alkaline earth dimers at the SCF approximation. They are stabilized by the attractive electron correlation forces.

At large distances, the electron correlation energy can be interpreted as a dispersion energy. At intermediate distances where the overlap of the atomic

Table IV: Comparison of E_2^{disp}, Eq. (10), with ΔE^{corr} for equilibrium and large distances, in kcal/mol.

	Be_2		Mg_2		Ca_2	
r,Å	E_2^{disp}	ΔE^{corr}	E_2^{disp}	ΔE^{corr}	E_2^{disp}	ΔE^{corr}
2.56	-79.62	-7.94				
3.92			-8.95	-2.27		
4.56					-14.40	-3.19
5.00	-0.35	-0.36	-1.29	-0.87	-6.85	-2.23
6.00	-0.10	-0.11	-0.35	-0.33	-1.68	-0.92
7.00	-0.03	-0.04	-0.11	-0.12	-0.55	-0.39
8.00			-0.04	-0.04	-0.22	-0.17
9.00					-0.10	-0.08
10.0					-0.05	-0.04

valence shells becomes essential, the dispersion forces cannot be defined without allowing for exchange effects. At these distances the multipole expansion is not valid [36]. It is instructive to compare the magnitudes of the pure dispersion energy and the electron correlation energy at different distances.

The energy of the dispersion interaction between two atoms can be presented with fine precision as a sum of three terms:

$$E_2^{disp} = -\left(\frac{C_6}{r^6} + \frac{C_8}{r^8} + \frac{C_{10}}{r^{10}}\right) \quad , \tag{10}$$

where the dipole-dipole (r^{-6}), dipole-quadrupole (r^{-8}), and dipole-octupole plus quadrupole-quadrupole (r^{-10}) dispersion interactions are taken into account. The dispersion coefficients C_n for the Be, Mg, and Ca atoms were estimated in Refs.[39] by the Padé approximant method. Using the values of C_n converted to $\left[\frac{\text{kcal}}{\text{mol}}\text{Å}^{\,n}\right]$ units, we have found the sum (10) at equilibrium

and at large distances and presented it in Table IV together with ΔE_{corr} calculated in Ref.[22]. As follows from Table IV, at large distances the electron correlation energy coincides with the pure dispersion energy with very good precision: for Be_2 at r $\geq$ 5 Å, for Mg_2 at r $\geq$6 Å, and for Ca_2 at r $\geq$9 Å. Note: this coincidence takes place for quantities calculated by different methods and at different approximations. From this follows that it is based on the physical ground: the dispersion forces have the electron correlation origin.

At equilibrium distances, the absolute value of the pure dispersion energy is much larger than ΔE_{corr} (in the case of Be_2, 10 times!). The exchange and overlap contributions to the electron correlation energy are repulsive and cause a decrease in dispersion attraction. At large distances, the dispersion energy in Ca_2 is about 5 times larger than that in Mg_2. This is correlated with the larger value of polarizability for the Ca atom compared with the Mg atom (Table I).

3.2 Trimers

In Table V we present the interaction energy at the SCF and MP4 levels for trimers Be_3, Mg_3, and Ca_3 in the equilateral triangle conformation. The trimers as well as dimers are not stable in the SCF approximation. According to Ref. [22], the SCF energy is positive at all calculated distances. On the other hand, the electron correlation corrections are negative and lead to stabilization of the alkaline-earth trimers. The binding in trimers is much stronger than in dimers. Especially in Be_3 where the value of E_b =25.9 kcal/mol is 14 times larger than the binding energy for Be_2 which has the van der Waals origin.

A more detailed analysis of the nature of binding is based on the many-body decomposition of the interaction energy

$$E_{int}^{MP4}(A_3) = E_2^{MP4}(A_3) + E_3^{MP4}(A_3) \tag{11}$$

which is also presented in Table V. The extremely large values of the ratio of the 3-body to 2-body energy for the equilibrium conformations of Be_3 and Mg_3 is connected with almost zero values of the 2-body interaction energies (the equilibrium distance in the Be_3 and Mg_3 equilateral triangle is located in the vicinity of the intersection of the $E_2(3)$ potential curve and the abscissa axis). Thus, in the frame of the many-body decomposition of the interaction energy, we have to conclude that for the Be_3 and Mg_3 trimers, the dominant factor of their stability are the 3-body forces. For the Ca_3 trimer the 2-body contribution to the interaction energy is non-negligible and amounts to 38%, although the 3-body interactions are a main contributor to the stability of the cluster.

Table V: Interaction energy and the many-body decomposition at the equilibrium geometry for the $C_{3\nu}$ symmetry, in kcal/mol.

Trimer	E_{int}^{MP4}	E_{int}^{SCF}	ΔE^{corr}	E_2^{MP4}	E_2^{SCF}	ΔE_2^{corr}	E_3^{MP4}	E_3^{SCF}	ΔE_3^{corr}	$\frac{E_3^{MP4}}{E_2^{MP4}}$
Be_3 $r_0 = 2.24$ Å	-25.90	0.60	-26.50	-0.79	35.45	-36.24	-25.11	-34.80	9.75	31.8
Mg_3 $r_0 = 3.32$ Å	-7.12	8.06	-15.18	-0.15	15.00	-15.15	-6.97	-6.94	-0.03	46.5
Ca_3 $r_0 = 4.12$ Å	-11.66	2.16	-13.82	-4.44	9.15	-13.59	-7.22	-6.98	-0.23	1.6

As discussed above, the equilibrium distances for the dimers are rather large, especially for Mg_2 and Ca_2. The addition of one more atom leads to a decrement in the equilibrium interatomic distance. In an equilateral triangle (the conformation which is the most stable conformation in the case of close-subshell-atom trimers) according to our calculations, the largest reduction 0.6 Å is revealed for Mg_3. However, for Be_3 and Ca_3, the reduction is also large enough: 0.32 Å and 0.44 Å, respectively. The explanation of this decrement is based on the interplay of the 2- and 3-body interactions in the cluster formation [6]: the attractive 3-body forces become larger with a decrease in the atom-atom distances while the 2-body forces undergo small changes because of the relative flatness of the 2-body potential curves.

In the same manner, as was done for the full interaction energy, the 2- and 3-body interaction energies can also be decomposed on the SCF and electron correlation parts:

$$E_n^{MP4} = E_n^{SCF} + \Delta E_n^{corr} \quad , n = 2, 3 \quad . \tag{12}$$

The 2-body SCF energy for an equilateral triangle is equal to

$$E_2^{SCF}(A_3) = 3E_{int}^{SCF}(A_2) \quad . \tag{13}$$

It indicates that, the physical sense of the 2-body SCF energy in trimers is the same as the SCF interaction energy in dimers: it is predominantly the exchange interactions which are repulsive for two interacting atoms with closed subshells. The attractive contributions from the electrostatic and induction energies are less than the repulsive exchange contribution. This is the reason that $E_2^{SCF}(A_3)$ is positive for the alkaline trimers in all calculated distance regions [22].

The situation is different in the case of the 3-body SCF energy. The main contribution to $E_3^{SCF}(A_3)$ is given by the 3-body exchange forces. These forces originate from the three-atomic electron exchange which mixes electrons of all three atoms. In closed-shell atom systems, contrary to the 2-body exchange forces, the 3-body exchange forces are attractive and make a contribution to the stabilization of trimers. Thus, for trimers there are two stabilization factors: ΔE_3^{SCF} and ΔE_2^{corr} .

The 2-body electron correlation energy, $\Delta E_2^{corr}(A_3)$, as in the case of dimers, is reduced at large distances to the dispersion energy. At intermediate distances, it contains both the exchange and dispersion contributions which cannot be separated. The exchange effects decrease the dispersion attraction; nevertheless, the 2-body electron correlation appears as a main factor of stabilization, especially for the Mg_3 and Ca_3 trimers.

The 3-body electron correlation energy, $\Delta E_3^{corr}(A_3)$, at large distances can be represented as the Axilrod-Teller 3-body dispersion energy [40]

$$E_3^{dis}(A_3)=\frac{C_9}{r_{ab}^3 r_{ac}^3 r_{bc}^3}(1+3Cos\theta_a Cos\theta_b Cos\theta_c) \quad . \tag{14}$$

For an equilateral triangle, Eq (14) is transformed to

$$E_3^{dis}(A_3) = \frac{11}{8}\frac{C_9}{r_{ab}^9} \tag{15}$$

According to Eq.(15), the 3-body dispersion energy is positive as is ΔE_3^{corr} at large distances. At intermediate distances, the negative contributions from the 3-body exchange and overlap effects can lead to negative values for ΔE_3^{corr}. This is what is revealed for Ca_3 and, close to the equilibrium distances, for Mg_3.

Note that the larger value of binding energy E_b (Ca_3) = 11.66 kcal/mol compared with E_b (Mg_3)=7.12 kcal/mol in spite of the greater equilibrium distance in the Ca_3 trimer is due to the smaller value of the repulsive SCF energy for Ca_3 : E_2^{SCF} (Ca_3)=9.15 kal/mol and E_2^{SCF} (Mg_3)=15 kcal/mol. This results in a greater stability of Ca_3 because the total attractive contribution for Ca_3 is smaller than for Mg_3 : $\Delta E_2^{corr} + E_3^{SCF} + \Delta E_3^{corr}$ = -20.8 and -22.12 kcal/mol for Ca_3 and Mg_3, respectively (see Table V).

3.3 Population of vacant atomic orbitals and electron density distribution

It is instructive to study the vacant atomic orbital population in dimers and trimers. As mentioned in the Introduction, in the 80's Bauschlicher et al. [10,11] came to the conclusion that the promotion of ns-electrons to np-orbitals leading to sp-hybridization is the main mechanism responsible for binding in alkaline-earth clusters. This conclusion was based on a study of the SCF Mulliken population analysis for tetramers, which are stable at the SCF level. At present, we can perform more precise analysis using the Natural Bond Orbital Analysis and calculate it at the electron correlation level.

In Table VI we present the net population of valence orbitals in dimers and trimers. We see that not only the p-population but even the d-population, especially for the Ca clusters, are not negligible. The latter is correlated with the experimental atomic excitation energies ΔE_{at} [24]. According to Table I, the energy of the 4s⟶3d excitation in the Ca atom is even smaller than the

Table VI: The net valence population, Δn_l^a, for the isolated atoms and clusters at the equilibrium geometry, obtained by the Natural Bond Orbital Analysis at the SCF and MP4 levels.

	SCF				MP			
A_n/l	ns	(n+1)s	np	nd	ns	(n+1)s	np	nd
Be	0.000	0.000	0.000	0.000	-0.135	0.004	0.130	0.001
Be_2	-0.044	0.006	0.037	0.001	-0.199	0.008	0.185	0.006
Be_3	-0.257	0.005	0.246	0.005	-0.315	0.009	0.288	0.016
Mg	0.000	0.000	0.000	0.000	-0.112	0.004	0.105	0.003
Mg_2	-0.007	0.001	0.005	0.000	-0.123	0.004	0.113	0.005
Mg_3	-0.045	0.002	0.040	0.002	-0.173	0.005	0.154	0.012
Ca	0.000	0.000	0.000	0.000	-0.138	0.003	0.124	0.011
Ca_2	-0.016	0.002	0.011	0.003	-0.161	0.005	0.139	0.018
Ca_3	-0.074	0.003	0.057	0.015	-0.229	0.006	0.184	0.039

[a]For atoms $\Delta n_l^{MP4}(A) = n_l^{MP4}(A) - n_l^{SCF}(A)$, for clusters $\Delta n_l^{MP4}(A_n) = n_l^{MP4}(A_n) - n_l^{SCF}(A)$, the similar definition is for n_l^{SCF}, therefore $n_l^{SCF}(A) = 0$.

ns⟶np excitation energies in Be and Mg atoms. On the other hand, there is no quantitative relation between ΔE_{at} and the net population numbers Δn_l in Table VI. The magnitude of ΔE_{at} (ns⟶np) in Be is larger than that in Ca; nevertheless, the np-population in the Be clusters is larger than in the Ca clusters.

We have also calculated the NBO valence population at the MP4 level for the isolated atoms. It could be expected that the inclusion of the electron correlation effects leads to some population of vacant (in the SCF approximation) atomic orbitals. But the values obtained are surprisingly large. The p-population in the Mg and Ca atoms are only slightly smaller than that in their dimers, and in the Be atom the population is 0.7 of the p-population in Be_2.

It is important to check: is the effect of a rather large population of vacant atomic orbitals at the electron correlation level specific for alkaline-earth atoms or it has a general character. In Table VII we present the results of net valence population calculations for noble-gas atoms performed by the Natural Bond Orbital Analysis at the MP4 level. We found non-negligible valence orbital population, especially for the d-orbitals. The results obtained for three different basis sets are quite close. Thus, the population of vacant orbitals in noble-gas atoms is not an artifact of the calculations. From this follows that elements traditionally assumed as closed-shell (noble gases) or closed-subshell (alkaline earths) atoms can to some extent manifest an anisotropic p- or d-symmetry behavior. It would be very interesting to obtain experimental evidence confirming this theoretical prediction.

Table VII: The net valence population, Δn_l^a, for isolated noble-gas atoms, obtained by the Natural Bond Orbital Analysis at the MP4 level.

atoms	ns	np	$\sum_m (n+m)s$	$\sum_m (n+m)p$	nd	nf
	a) The Sttutgart / Dresden basis set [41]					
Ne	-0.011	-0.062	0.009	0.040	0.023	0.002
Ar	-0.019	-0.129	0.007	0.028	0.105	0.008
Kr	-0.018	-0.119	0.006	0.024	0.095	0.012
Xe	-0.020	-0.131	0.006	0.021	0.106	0.019
	b) The Stevens et al. basis set [42,43]					
Ne	-0.010	-0.060	0.008	0.037	0.023	0.002
Ar	-0.019	-0.130	0.007	0.026	0.107	0.008
Kr	-0.018	-0.123	0.006	0.023	0.100	0.012
Xe	-0.020	-0.134	0.006	0.020	0.109	0.019
	c) 6-311+G (3df) basis set [44]					
Ne	-0.010	-0.061	0.008	0.039	0.022	0.002
Ar	-0.018	-0.126	0.007	0.027	0.101	0.009
Kr	-0.018	-0.119	0.006	0.024	0.095	0.012
Xe	no basis set available					

[a] $\Delta n_l(A) = n_l^{MP4}(A) - n_l^{SCF}(A)$

We have to take into consideration that some atom-atom interactions, which enhance the excited orbital population, do not lead to a bonding state. The last statement is confirmed by the valence orbital population in the alkaline-earth clusters at the SCF level. According to Table VI, at the SCF level there is a non-negligible p-population, especially for trimers. But in the

SCF approximation, the dimers and trimers are not stable. Thus, the repulsive SCF interactions also lead to the vacant orbitals population, although this kind of hybridization does not lead to binding.

The calculations in Ref. [10] were performed at the SCF level. In the frame of the latter, the isolated atoms do not have populated excited orbitals. The authors [10] found the ratio of p-population in different tetramers (which are stable at the SCF level) proportional to the ratio of their dissociation energies. However, at an election correlation level because of the p-population in the isolated atoms, we cannot expect such proportionality. It is evident for dimers: the p-population is largest in Be_2, although the bond strength is largest in Ca_2. For dimers, the p-population is not very different from that in the isolated atoms whereas for trimers the increase of the p-population is rather large. It is not directly proportional to the bond strength, but its amount qualitatively reflects a trend toward a more strong bond formation by the sp-hybridization.

More insight into the bonding comes from the density difference maps. The partitioning of the total density difference into 2- and 3- body terms was performed in the analogy to interaction energy expressions. In Figs. 1 and 2 we present the total density difference maps and its 2- and 3-body contributions in the Be_3 plane and in the perperdicular plane passing through the Be-Be bond. For 2-body density difference, we have positive values along the Be-Be bond which can be attributed to the σ-type bonding (the latter is more clear from the plot in the plane perpendicular to the Be_3 plane, Fig. 2a). The 2-body dispersion interactions do not change the density distribution. Thus, the σ-type redistribution originates from the SCF 2-body interactions, inside which there are two attractive interactions: electrostatic and induction. Because of the larger 2-body exchange repulsion, these attractions are not sufficient for the stabilization of Be_3, and we have to conclude that the σ-type redistribution of the 2-body density difference does not lead to a real bonding. This is analogical to the atomic p-population at the SCF level which also does not lead to trimer stability.

Figs. 1a and 2a also reveal a positive density difference in the nonbonding region (the area outside the atoms attached to the vertices of the triangle Be_3). This reflects the antibonding character of the 2-body exchange interactions. The 3-body interactions shift the electron density from nonbonding to bonding regions because in the total density difference plots, the electronic density gain is observed only in the bonding area (Fig. 1c).

As follows from Fig. 1b and 2b, the 3-body density difference is positive outside of the Be-Be line in a direction perpendicular to it, whereas it is negative beyond the Be_3 plane. So, the density difference has the π-in-plane character but is shifted outside the triangle Be3. The total density difference

plot (Fig 1c) resembles the interstitial orbital picture obtained in Li_N clusters by spin-coupled valence bond method [45,46]. This can also be connected with the rather large p-population of Be atoms in trimers.

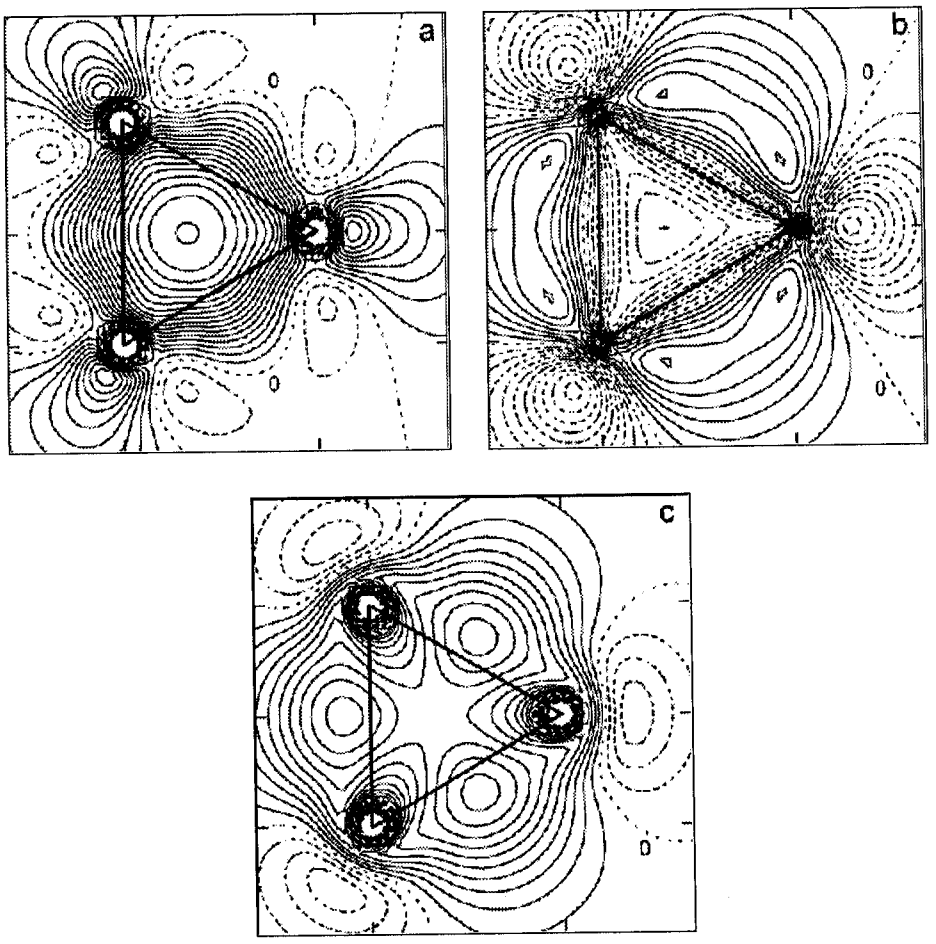

Figure 1: The electronic density difference maps for the Be_3 trimer partitioned for 2-body (a) and 3-body (b) contributions and the total difference density distribution (c). The plot is done in the plane of Be_3. The spacing between the contours is 0.001 electron/bohr. The contour with no density charge are labeled with zeros while solid lines indicate the enhancement of electronic density.

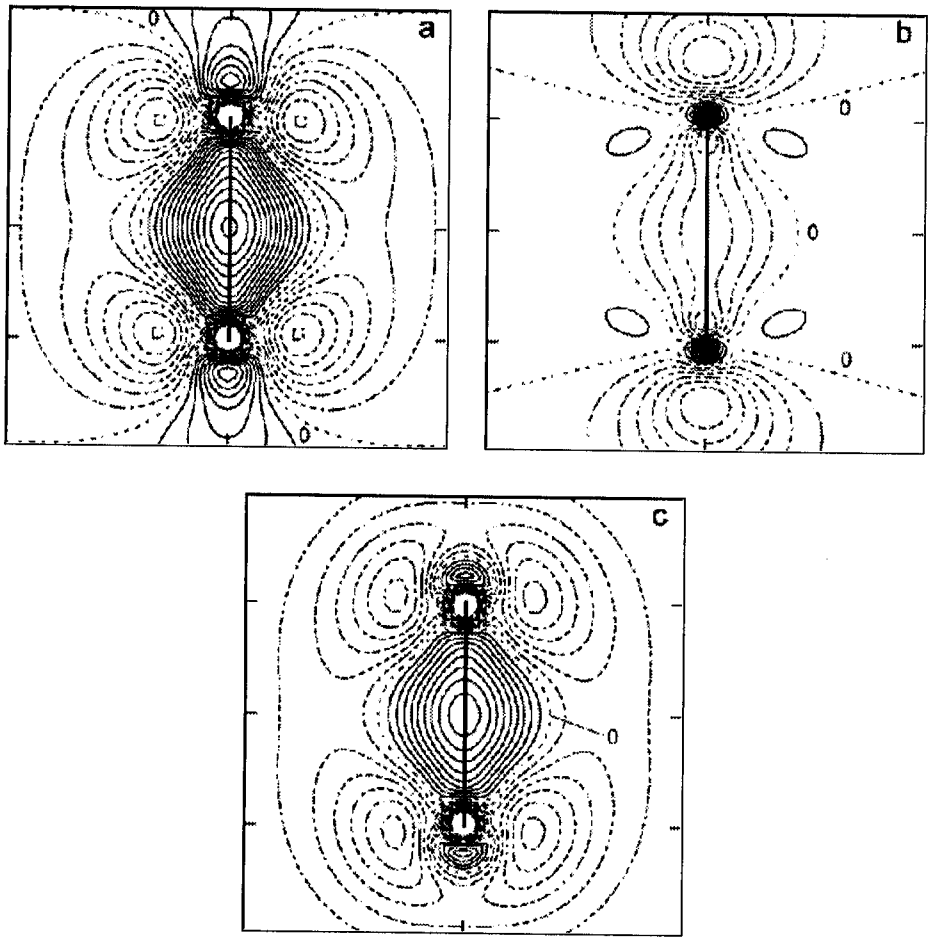

Figure 2: The electronic density difference maps for the Be_3 trimer partitioned for 2-body (a) and 3-body (b) contributions and the total difference density distribution (c). The plot is done in the plane perpendicular to the Be_3 plane and passing through the Be-Be bond. The spacing between the contours is 0.001 electron/borh. The contours with no density charge are labeled with zeros while solid lines indicate the enhancement of electronic density.

ACKNOWLEDGEMENT

This work was facilitated in part by the projects IN108697 of DGAPA UNAM and 32227- E of CONACYT (Mexico), the U.S. NSF grant 9805465, Wroclaw University of Technology Grant No. 341-831, and the U.S. Army High Performance Computing Research Center under the auspices of the Department of Army, Army Research Laboratory cooperative agreement number DAAH04-95-2-0003/contract number DAAH04-95-C-0008. This work does not necessarily reflect the policy of the USA government, and no official endorsement should be inferred. We would like to thank the Mississippi Center for Supercomputing Research, Poznan and Wroclaw Supercomputing and Networking Centers, and the Interdisciplinary Center for Mathematical and Computational Modeling of Warsaw University for a generous allotment of computer time.

References

[1] I.G. Kaplan, Int. J. Quant. Chem. **74**, 241, (1999).

[2] F. Luo, G. Kim, G.C. Mc Bane, C.F. Giese, and W.R. Gentry, J. Chem. Phys. **98**, 9687, 10086 (1993).

[3] W. Kolos, F. Nieves, and O. Novaro, Chem. Phys. Lett. **41**, 431 (1976).

[4] O. Novaro and W. Kolos, J. Chem. Phys. **67**, 5066 (1977).

[5] J.P. Daudey, O. Novaro, W. Kolos, and M. Berrondo, J. Chem. Phys. **71**, 4297 (1979).

[6] I.G. Kaplan, J. Hernández-Cobos, I. Ortega-Blake, and O. Novaro, Phys. Rev. **A53**, 2493 (1996).

[7] I.G. Kaplan, Adv. Quantum. Chem. **31**, 137 (1999).

[8] J. Hernández-Cobos, I.G. Kaplan, and J.N. Murrell, Mol. Phys. **92**,63 (1997).

[9] I.G. Kaplan, Polish J. Chem. **72**, 1454 (1998).

[10] C.W. Bauschlicher, V. Bagus, and B.N. Cox, J. Chem. Phys. **77**, 4032 (1982).

[11] S.P. Walch and C. W. Bauschlicher, J. Chem. Phys. **83**, 5735 (1985).

[12] R.J. Harrison and N.C. Handy, Chem. Phys. Lett. **123**, 321 (1986).

[13] V. Reuse, S. N. Khanna, V. De Coulon, and J. Buttet, Phys. Rev. **B39**, 12911 (1989); **B41**, 11743 (1990).

[14] T.J. Lee, A.P. Rendell, P. Rendell, and P.R. Taylor, J. Chem. Phys. **93**, 6636 (1990).

[15] T.J. Lee, A.P. Rendell, and P.R. Taylor, J. Chem. Phys. **92**, 489 (1990).

[16] J.D. Watts, I. Cernusak, J. Noga, R.J. Bartlett, C. W. Bauschlicher, Jr. T.J. Lee, A. P. Rendell, and P.R. Taylor, J. Chem. Phys. **93**, 8875 (1990).

[17] T.J.Lee, A.P. Rendell, and P.R. Taylor, Theor. Chim. Acta, **83**, 165 (1992).

[18] W. Klopper and J. Almlöf, J. Chem. Phys. **99**, 5167 (1993).

[19] P.V. Sudhakar and K. Lammertsmaa, J. Chem. Phys. **99**, 7929 (1993).

[20] L.A. Ericksson , J. Chem. Phys. **103**, 1050 (1995).

[21] E.R. Davidson and R.F. Frey, J. Chem. Phys. **106**, 2331 (1997).

[22] I.G. Kaplan, S. Roszak, and J. Leszczynski, J. Chem. Phys. **113**, 6245 (2000).

[23] CRC Handbook of Chemistry and Physics, Ed. D.R. Leed, 74th Edition CRC Press: Boca Raton 1993-1994.

[24] C.E. Moore, "Atomic Energy Levels," vol. I, Circular of the NBS 467, Washington, 1949.

[25] C. F. Bunge, J. A. Barrientos, and A. Vivier-Bunge, Atomic Data and Nuclear Data Tables **53**, 113 (1993).

[26] C. Kittel, "Introduction to Solid State Physics," Wiley & Sons: New York, 1996, 7th Edition, p. 57.

[27] V. E. Bondybey, Chem. Phys. Lett. **109**, 436, (1984).

[28] A. E. Balfour and A. E. Duglas, Can. J. Phys. **48**, 901 (1970).

[29] C.R. Vidal and H. Scheingraber, J. Mol. Spectr. **65**, 46 (1977).

[30] Gaussian 98, Revision A.6, M.J. Frisch, G. W. Trucks, H.B. Schlegel, G. E. Scuseria, M. A. Robb, J.R. Cheeseman, V. G. Zakrzewski, J. A. Montgomery, Jr. Stratmann, R. E., J. C. Burant, S. Dapprich, J.M. Millam, A.D. Daniels, K. N. Kudin, M.C. Strain, O. Farkas, J. Tomasi, V. Barone, M. Cossi, R. Cammi, B. Mennucci, C. Pomelli, C. Adamo, S. Clifford, J. Ochterski, G.A. Petersson, P. Y. Ayala, Q. Cui, K. Morokuma, D.K. Malick, A.D. Rabuck, K. Raghavachari, J.B. Foresman, Cioslowski, J. V. Ortiz, B.B. Stefanov, G. Lui, A. Liashenko, P. Piskorz, I.J. Komaromi, R. Gomperts, R.L. Martin, D.J. Fox, T. Keith, M.A. Al-Laham, C.Y. Peng, A. Nanayakkara, C. Gonzalez, M. Challacombe, P.M.W. Gill, B. Johonson, W. Chen, M. W. Wong, J.L. Andres, C. Gonzalez, M. Head-Gordon, E.S. Replogle, and J.A. Pople, Gaussian, Inc., Pittsburgh PA, 1998.

[31] F.W. Biegler-König, R.F.W. Bager, and T.H. Tang, J. Comput. Chem. **3**, 317 (1982).

[32] K.B. Wiberg, C.M. Hadad, T.J. Le Page, C.M. Breneman, and M.J. Frisch, J. Phys. Chem. **96**, 671 (1992).

[33] A.E. Reed, L.A. Curtiss, and F. Wienhold, Chem. Rev. **88**, 899 (1988).

[34] G.D. Purvis and R.J. Bartlett, J. Chem. Phys. **76**, 1910 (1982).

[35] J.A. Pople, M. Head-Gordon, and K. Raghavachari, J. Chem. Phys. **87**, 5968 (1987).

[36] I.G. Kaplan, Theory of Molecular Interactions (Elsevier, Amsterdam, 1986).

[37] K. Kitaura and K. Morokuma, Int. J. Quant. Chem. **10**, 325 (1976).

[38] G. Chalasinski, M.M. Szczesniak, and S.M. Cybulski, J. Chem. Phys. **92**, 2481 (1990).

[39] J.M. Standart and P.R. Certain, J. Chem. Phys. **83**, 3002 (1985).

[40] B.M. Axilrod and E. Teller, J. Chem. Phys. **11**, 299 (1943).

[41] A. Bergner, V.M. Dolg, W. Kuechle, H. Stall, and H. Preuss, Mol. Phys. **80**, 1431, (1993).

[42] W.J. Stevens, H. Basch, and M. J. Krauss , Chem. Phys. **81**, 6026, (1984).

[43] W.J. Stevens, M. Krauss, H. Basch, and P.G. Jasien , Canad. J. Chem. **70**, 612, (1992).

[44] L.A. Curtiss, M.P. Mc Grath, J-P. Blandeau, N.E. Davis, R.C. Binning, Jr, and L. J. Radom Chem. Phys. **103**, 6104, (1995).

[45] E. Tornaghi, D.L. Cooper, J. Gerratt, and M. Raimondi, J. Mol. Struct. (Theochem) **259**, 383, (1992).

[46] E. Tornaghi, D.L. Cooper, J. Gerratt, and M. Raimondi, J. Chem. Soc. Farad. Trans. **88**, 2309, (1992).